Whitmarsh, R.B., Sawyer, D.S., Klaus, A., and Masson, D.G. (Eds.), 1996
Proceedings of the Ocean Drilling Program, Scientific Results, Vol. 149

25. MAGNETIC SIGNATURES OF PERIDOTITE ROCKS FROM SITES 897 AND 899 AND THEIR IMPLICATIONS[1]

Xixi Zhao[2]

ABSTRACT

A paleomagnetic and rock magnetic study has been performed on the serpentinized peridotites recovered from Ocean Drilling Program Leg 149 Sites 897 and 899 across the ocean/continent transition in the Iberia Abyssal Plain to estimate the ages of their emplacement and subsequent alteration, which have a direct relation to the early opening of the North Atlantic. Stepwise thermal and alternating-field demagnetization experiments on 69 10-cm^3 minicore samples from Holes 897D and 899B show that the natural remanent magnetization (NRM) of many samples is composed mainly of a single stable component. The mean NRM intensity is typically on the order of 0.2 A/m for samples from Hole 897D, but about 1.3 A/m for samples from Hole 899B. The much stronger magnetization intensity of Site 899 is apparently in excellent agreement with a magnetic anomaly high observed in the vicinity of Site 899, suggesting that the serpentinized peridotite body under Site 899 contributes significantly to the magnetic anomaly. Conversely, the fact that Site 897 is located more oceanward but has a mean NRM intensity less than one-third of the average intensity (~4 A/m) of dredged and drilled oceanic basalts in the Atlantic may be used to explain the weakly negative anomaly data observed nearby.

At both sites, the upper part of the basement section immediately underlying the Pleistocene to Lower Cretaceous sedimentary cover is a zone of alteration in which rocks are pervasively veined and altered to brown-colored, altered, serpentinized peridotites. The lower part of the basement section consists of "fresher" greenish gray serpentinized peridotites. In this fresher lower part, the inclinations of characteristic magnetization show a consistent polarity pattern in a depth zone of about 20 m that is correlative between the two sites. Within this zone, the inclinations of samples are predominantly reversed, which is compatible with a reversed event (probably correlated to marine Anomaly M0 at about 118 Ma) prior to the Cretaceous Long Normal Superchron (84—118 Ma) and is incompatible with a Holocene field direction. In contrast, the inclinations of samples from the more "oxidized" upper part are almost all normal and the directions are similar throughout this part regardless of depth and lithology. This polarity pattern would suggest that the emplacement of these peridotites took place sometime during the middle Cretaceous (probably at the M0 time) and alteration of the upper part probably occurred during the Cretaceous Long Normal Superchron by convecting seawater during the opening of the North Atlantic. Paleomagnetic results from this study provide an example of the potential value of magnetic polarity dating of tectonic processes that accompanied continental breakup and the onset of steady-state seafloor spreading.

INTRODUCTION

It is well known that the ocean floor is not everywhere made of mafic rocks but also consists locally of serpentinized peridotites. Proposed models for the presence of the peridotites at, or close to, the seafloor are still debated. Many questions remain pertaining to the emplacement mechanisms of the peridotites. In general, peridotite occurrences can result from original mantle upwelling processes or from crystal fractionation in the layered gabbro zone that is immediately above the upper mantle. In places where the oceanic crust is very thin, such as along transform faults or along ridge valleys of slow-spreading ridges, it is quite possible that peridotites can be carried directly onto the oceanic floor by motion along normal faults (Bonatti and Honnorez, 1976; Girardeau et al., 1988). Such a mechanism has been proposed to explain the uplift of the peridotites recovered along ridges or transform fault segments of ridges. On the other hand, hot mantle uplift during continental rifting or asthenospheric vertical diapirism has been proposed to explain the original ascent of peridotites exposed on Zabargad Island (Nicolas et al., 1985, 1987; Bonatti et al., 1986), in the Alps (Nicolas, 1984), in the Betics (Obata, 1977; Tubia and Cuevas, 1977), and in the Pyrenees (Vielzeuf and Kornprobst, 1984). To explain the peridotites cropping out at the boundary between continents and oceans, Boillot et al. (1987) proposed that the rise of peridotites to the surface can result simply from tectonic denudation of the mantle as a consequence of stretching of the lithosphere during rifting. Beslier et al. (1990) further suggested that under the tectonic denudation model peridotite emplacement is strongly influenced by the extensional stress field at the end of continental rifting. At present, evidence from petrologic and fabrics studies of the peridotites alone cannot discriminate among various models. Additional geological and geophysical data are needed.

Another inherent problem in the investigation of peridotites is the determination of their precise ages. This stems largely from the absence of biostratigraphic dating and correlation in peridotites. An added problem is that most recovered peridotite has suffered extensive low-temperature and late-stage alteration, as typically evidenced by calcite veining as well as replacement of the serpentine by calcite, which makes it difficult to apply radiometric dating methods to these peridotites.

Paleomagnetism has proved to be a powerful tool in studying stratigraphic, tectonic, paleoclimatic, and paleoceanographic problems, and it continues to play a pivotal role as a standard for age-dating and correlation in Ocean Drilling Program (ODP) studies. Paleomagnetic dating is based on the facts that the Earth's magnetic field occasionally reverses polarity and that many rocks retain a magnetic imprint of the field at the time they were formed or altered. Under favorable circumstances, paleomagnetic dating can furnish highly resolved numerical ages by identifying the polarity patterns and fitting the polarity patterns into biostratigraphically identified zones, the geomagnetic polarity time scale, or other geochrological framework.

In this paper, I present a detailed account of paleomagnetic and rock magnetic results from the peridotite samples from Holes 897D and 899B drilled during Leg 149. By combining the paleomagnetic results with other available geological data, useful constraints can be

[1]Sawyer, D.S., Whitmarsh, R.B., Klaus, A., and Masson, D.G. (Eds.), 1996. *Proc. ODP, Sci. Results,* 149: College Station, TX (Ocean Drilling Program).
[2] Institute of Tectonics and Department of Earth Sciences, University of California, Santa Cruz, CA 95064, U.S.A. xzhao@earthsci.ucsc.edu

placed on the timing of emplacement and the postemplacement alteration of the recovered peridotites. This information may further our understanding of the processes that accompanied continental breakup and the onset of steady-state seafloor spreading.

GEOLOGICAL SETTING AND PETROGRAPHIC DESCRIPTION

Five sites were drilled during Ocean Drilling Program (ODP) Leg 149 at the ocean/continent transition west of Portugal (Fig. 1). Of these sites, Holes 897D and 899B of Sites 897 and 899, respectively, reached acoustic basement, and a sequence of serpentinized peridotite and associated mantle rocks was recovered from the basement. At Site 897, which is situated in the ocean/continent transition over a north-south basement ridge that has been linked to a peridotite ridge drilled west of Galicia Bank 140 km to the north (see Fig. 1), cores were obtained from three holes, which penetrated up to 694 m of Pleistocene to Lower Cretaceous sediments and up to 153 m of basement. Site 899 lies within the same part of the ocean/continent transition and is about 20 km east of Site 897. At Site 899, 563 m of upper Pliocene to Upper Cretaceous sediment overlying the serpentinized peridotites were penetrated in two holes (Fig. 2).

The peridotite recovered during Leg 149 has suffered extensive low-temperature and late-stage alteration, which includes serpentinization, serpentine and calcite veining, and replacement by calcite. The two most obvious visible features resulting from this alteration are color variation and calcite veining. At both sites, the upper part of the peridotite section immediately underlying the Pleistocene to Lower Cretaceous sedimentary cover is pervasively veined and altered to a brown-colored serpentinized peridotite and breccia. The finer grained matrix within the upper part is dominantly dark yellowish brown (10YR 4/2) to moderate yellowish brown (10YR 5/4). The lower part of the peridotite section consists of "fresher" (compared with that of the upper part of the section) serpentinized peridotites, which are generally dark green (5GY 4/1) or greenish black (5G 2/1). At both holes, Lower Cretaceous (upper Hauterivian) claystone and siltstone are found at the bottom of the basement section (see Fig. 2), although these sediments in Hole 897D are relatively minor compared with those of Hole 899B. Preliminary shipboard geochemical studies indicate that originally the peridotite section was relatively uniform in composition, but that now the "altered" rocks in the upper part are significantly enriched in $CaCO_3$, Sr, Ba, P, K, and V, but depleted in Mg, Fe, and Si relative to the underlying fresher greenish peridotites (Sawyer, Whitmarsh, Klaus, et al., 1994). Conversely, elements such as Ni and Cr, abundant in the unaltered fresher lower part of the section, are depleted in the altered upper part. Shear textures of the altered peridotites within the upper part of the section are confined to basal margins of these rocks, suggesting they formed at shallow depth during the addition of seawater (Seifert et al., 1993). Relict mineral and X-ray fluorescence data indicate that the peridotites were dominantly lherzolite with lesser amounts of harzburgite and dunite.

PALEOMAGNETIC SAMPLING AND MEASUREMENTS

All cores from Holes 897D and 899B were drilled using the rotary core barrel (RGB). Therefore, these cores were not oriented with respect to north. A total of 69 minicore samples (each with diameter 2.5 cm, length 2.2 cm) were taken from Holes 899B (36) and 897D (33) using a water-cooled nonmagnetic drill bit attached to a standard drill press. The samples were taken from long and continuous pieces of core sections so as to exclude those that had flipped over inside the drilling pipe, thus ensuring that the inclinations of the samples were not disturbed. The depth, freshness, color, and the general appearance

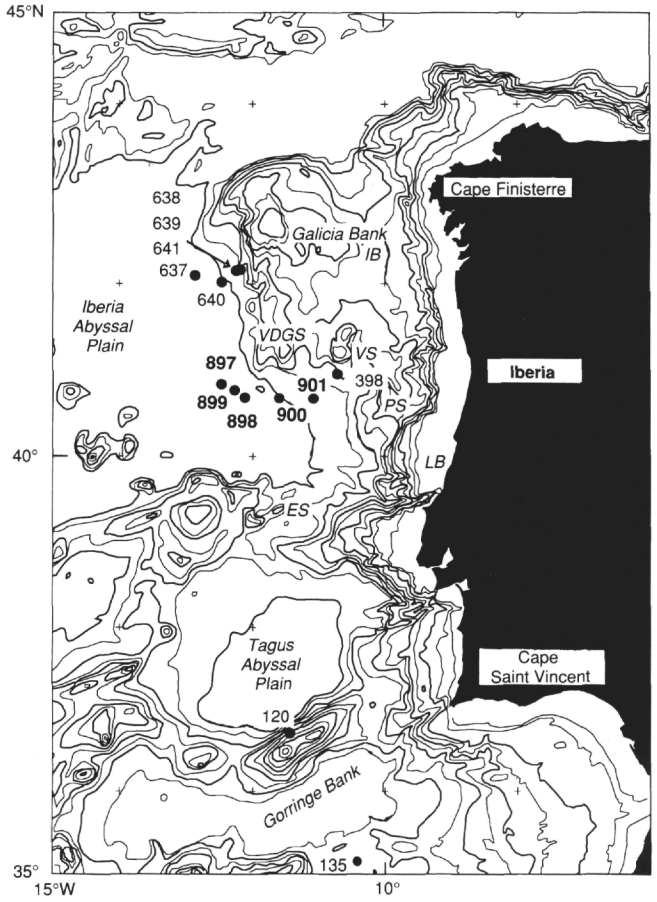

Figure 1. Regional bathymetric chart of the west Iberia Margin (contours in 500-m intervals, 1000-m contours in bold). Smaller numbers refer to previously drilled DSDP/ODP sites; larger, bold numbers refer to sites drilled during Leg 149. IB = Interior Basin, VDGS = Vasco da Gama Seamount, VS = Vigo Seamount, PS = Porto Seamount, LB = Lusitanian Basin, ES = Estremadura Spur.

of each sample were carefully registered. This sampling procedure facilitated the process of comparing the paleomagnetic results of individual samples with the corresponding core photographs and assessing the validity of the paleomagnetic results in a reliable manner. After splitting individual pieces of the core, ODP workers follow the same convention in handling rotary cores as for an oriented piston core (Fig. 3). Magnetic measurements were performed mainly with a 2G cryogenic magnetometer and a Schonstedt spinner magnetometer in the paleomagnetic laboratory at the University of California at Santa Cruz, but a few samples were measured during the cruise with Schonstedt and Molspin equipment. As the shipboard measurements revealed that these peridotites are highly susceptible to a magnetic field, subsequent shore-based demagnetization experiments were done in a zero-field paleomagnetic laboratory using Schonstedt equipment and a customized thermal demagnetization oven. For each sample, a vector plot of the directions of the magnetization during progressive demagnetization was analyzed to obtain the characteristic component (ChRM) and its polarity. Magnetic components, linear in three-dimensional space, were determined by fitting least-squares lines to segments of the vector demagnetization plots or by using "principal component analysis" methods (Zijderveld, 1967; Kirschvink, 1980). Bulk magnetic susceptibility and anisotropy of magnetic susceptibility (AMS) were measured using a Kappabridge KLY-2 (Geofyzika Brno). The susceptibility tensor (K_{ij}) of each sample was calculated from the measurements in 15 positions. Several samples were subjected to 20-mT

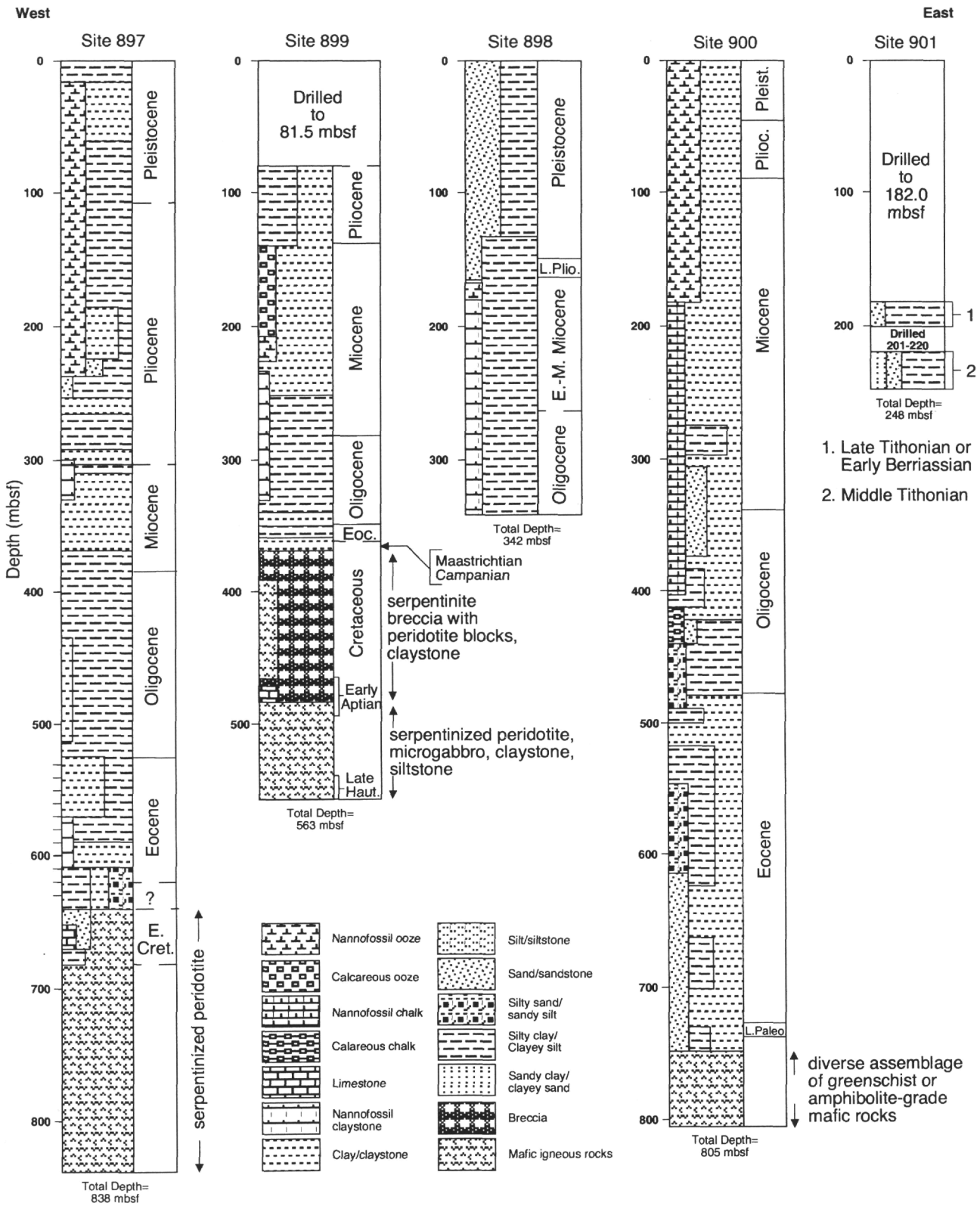

Figure 2 . Summary lithologic columns from the five sites drilled during Leg 149 in the Iberia Abyssal Plain.

demagnetization with tumbling alternating field (AF) demagnetizer prior to AMS measurement in order to remove the scatter due presumably to AMS dependent on natural remanent magnetization (NRM). To avoid potential problems associated with heating (Rochette et al., 1992), the AMS measurement was completed before any thermal demagnetization experiments were conducted.

RESULTS

The paleomagnetic results of the peridotites from the two holes are summarized in Tables 1 and 2. The most common features are outlined below.

Natural Remanent Magnetization

The NRM intensities of the peridotites (Tables 1, 2) range from 14 to 924 mA/m in Hole 897D and from 290 to 2455 mA/m in Hole 899B. In both holes, the intensities become stronger in the lower part of the peridotite section (772.18-819.48 m below seafloor [mbsf] in Hole 897D and 475.10-511.56 mbsf in Hole 899B). Although the intensity in Hole 899B is scattered (Fig. 4), the peaks and lows in the downhole profile appear to coincide with petrographical boundaries in the section. In Hole 897D, the remanence successively shows a steplike decrease at first and then increases with depth. In detail, it follows three trends: (1) from 694.49 through 754.86 mbsf, the NRM intensities are scattered with a mean of 296 mA/m; (2) from 755.81 through 763.24 mbsf, the intensities are much weaker (mean 33 mA/m); and (3) from 772.69 through 828.40 mbsf, the intensities are stronger (mean = 394 mA/m) and more scattered (Fig. 4).

Demagnetization Behavior

One of the major experimental requirements in paleomagnetic research is to isolate the characteristic remanent magnetization by selective removal of secondary magnetization. As shown in Figure 5, thermal demagnetization on Samples 149-899B-23R-1, 12-14 cm, and 149-897D-16R-2, 72-74 cm (both from the fresher lower part of the section) removed a "soft" component, probably of viscous origin, at low to intermediate temperatures (200°-400°C). Up to 585°-620°C demagnetization, the magnetization revealed the stable component of magnetization. In the altered upper part, however, most samples show a single component of magnetization during demagnetization (Fig. 6). In addition, it appears that there is no significant difference in demagnetization behavior of peridotite samples throughout this part of the section whether samples are from the matrix, clasts, or even veins. Examples of this behavior are shown in Figure 6: Sample 149-899B-20R-2, 112-114 cm, which was specifically chosen from a heavily veined piece of core, exhibited magnetic properties identical to veinless Sample 149-899B-21R-2, 75-77 cm.

Although in general a stable component of magnetization can be identified by both thermal and AF demagnetization techniques (Figs. 5, 6), the removal of secondary magnetization was better accomplished through thermal demagnetization than through AF demagnetization. The dominant magnetic mineral in these peridotites appears to be magnetite as indicated by the unblocking temperatures and coercivities. The magnetically cleaned inclinations from both holes are systematically shallower than the expected inclinations at the drilling sites, assuming that Iberia has been part of stable Europe since the Cretaceous. The discrepancy in inclination (about 25°) may indicate that Iberia had a microplate nature at the time of acquisition of the magnetization. As discussed later, Iberia is indeed believed to have been independent plate in the Cretaceous.

Magnetic Susceptibility and Koenigsberger Ratio

The magnetic susceptibility *(K)* is controlled by the volume concentration of ferromagnetic minerals as well as by grain size and other parameters such as stress. The magnetic susceptibility of Hole 899B (mean 2.959×10^{-2} SI units) is about 1.4 times higher than that of Hole 897D (mean 2.067×10^{-2} SI units). Although the scatter in susceptibility is less than that of the NRM intensities, the susceptibility values show a pattern similar to the NRM intensities (Fig. 7).

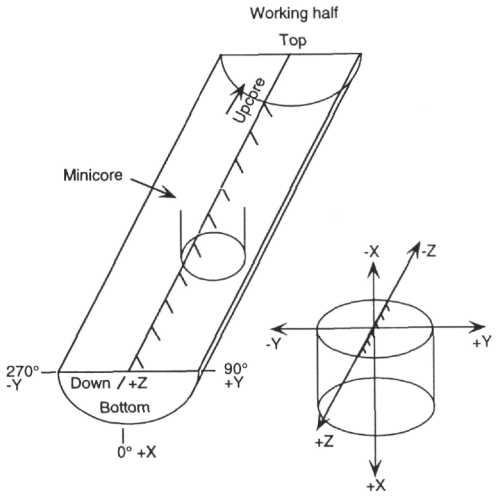

Figure 3. ODP core conventions used in this study.

The Koenigsberger ratio *(Q* ratio) is defined as the ratio in a rock of remanent magnetization to the induced magnetization in the Earth's field:

$$Q = NRM\ (\text{A/m}) / (K\ (\text{SI}) \bullet H\ (\text{A/m}), \quad (1)$$

where K is the magnetic susceptibility in SI units and H is the local geomagnetic field (the International Geomagnetic Reference Field value at the Leg 149 sites [45,000 nT = 35.83 A/m] was used for calculating *Q).* In general, the Koenigsberger ratio is used as a measure of stability to indicate a rock's capability of maintaining a stable remanence.

The distribution of the Koenigsberger ratios in both holes (Fig. 8) resembles that of the NRM. Although the mean susceptibility values of the two holes are comparable, Hole 899B has a higher mean intensity of the remanence, and consequently, the Koenigsberger ratio of Hole 897D (mean 0.423) is lower than that of the Hole 899B (mean 2.049). Within the altered upper part section in Hole 899B, a sharp increase in the Koenigsberger ratio occurs at 421.93 mbsf (Sample 149-899B-21R-4, 97-99 cm). A similar spike is also present in Hole 897D (Sample 149-897D-13R-1, 62-64 cm). The Koenigsberger ratio peaks in both holes may serve as one of the stratigraphic markers for these two sites (the significance of this peak is discussed in more detail later and is summarized in Table 3). The *Q* ratio is less than 1.0 in all but two of the samples in Hole 897D, whereas in Hole 899B it is normally close to or slightly greater than 1.0 (with only four exceptions). The low values of the *Q* ratio demonstrate that induced magnetization would either dominate or be comparable to that of the remanent magnetization if present in an external magnetic field. This underscores the importance of measuring these rocks in a field-free room at the shore-based laboratory.

Anisotropy of Magnetic Susceptibility

AMS is a physical property of rocks that is used for petrofabric and structural studies. It measures the sum of the anisotropies of the individual minerals in a rock. AMS results can be described by an ellipsoid of magnetic susceptibility, with dimensions defined by the magnitudes of the principal susceptibilities. These lie along the three orthogonal axes of the ellipsoid and are designated the maximum, in-

Table 1. Magnetic properties of peridotite recovered from Hole 899B.

Core, section, interval (cm)	Depth (mbsf)	NRM intensity ($\times 10^{-1}$ A/m)	Declination (°)	Inclination (°)	K ($\times 10^{-6}$ SI)	Q ratio	$P = K_1/K_3$
149-899B-							
16R-2, 13–15	371.25	12.06	158.8	12.2	24590	1.369	1.036
16R-3, 57–59	372.96	8.24	195.5	20.4	17970	1.28	1.013
17R-1, 86–88	380.26	12	155.2	16.4	23460	1.428	1.016
17R-2, 4–6	380.87	7.38	200.5	12.4	21220	0.971	1.031
18R-1, 66–68	389.76	21.15	190.7	61.7	47060	1.254	1.064
18R-3, 57–59	392.22	8.76	206.8	−7.6	20060	1.219	1.021
18R-4, 15–17	393.28	8.2	184	10.5	23030	0.994	1.013
18R-5, 8–10	394.32	16.14	207.2	20.2	27410	1.643	1.028
19R-1, 24–26	398.51	21.66	5.1	−16.7	39570	1.528	1.071
19R-3, 70–72	401.85	22.45	169.6	57.5	73770	0.849	1.19
19R-4, 1–3	402.25	15.27	188.9	9.7	35700	1.194	1.153
20R-2, 112–114	410.32	11.29	211.6	17.2	8081	3.899	1.143
21R-1, 64–66	417.74	19.92	168.7	21.3	30290	1.835	1.093
21R-2, 75–77	418.99	7.29	188.7	26.7	7078	2.875	1.172
21R-3, 57–59	420.05	3.09	203.7	3.7	1509	5.715	1.058
21R-4, 97–99	421.93	8.89	161.2	50.7	1048	23.68	1.141
21R-5, 43–45	422.85	15.54	148.7	−6.8	27450	1.58	1.026
22R-1, 134–136	427.64	11.53	193.1	12.8	27970	1.151	1.043
22R-2, 27–29	428.03	21.76	228.9	−44	62650	0.969	1.147
23R-1, 4–6	435.64	11.56	163.1	29.6	27420	1.177	1.016
23R-1, 12–14	435.72	14.08	193	−23.1	32410	1.213	1.019
23R-4, 16–18	440.14	6.71	193.4	−26.9	20450	0.916	1.013
24R-1, 38–40	445.68	3.31	181.6	−33.8	16310	0.566	1.02
24R-2, 33–35	447.13	14.2	196.5	9.5	26390	1.502	1.038
24R-3, 121–123	449.47	12.88	191.6	−13	31770	1.132	1.023
25R-1, 67–69	455.37	6.16	197.9	13.2	23270	0.739	1.024
25R-3, 29–31	457.76	14.36	181.6	−17.8	36320	1.103	1.027
25R-3, 34–36	457.81	14.23	181.7	−23.3	40500	0.981	1.057
26R-1, 26–28	464.46	24.55	190.5	16.2	40850	1.677	1.062
26R-1, 60–62	464.8	13.71	184.1	12.6	33930	1.128	1.015
27R-2, 2–4	475.1	7.89	114.4	−25.3	34070	0.646	1.031
28R-1, 106–108	483.96	2.9	359.7	−22	34960	0.232	1.261
28R-2, 0–2	484.35	6.06	160.8	24.7	13360	1.266	1.01
29R-1, 118–120	493.28	22.17	176.4	48.8	40710	1.54	1.049
30R-1, 99–101	502.99	19.55	252.7	−79.7	42330	1.289	1.067
30R-2, 21–23	503	15.6	117.4	67.6	50230	0.867	1.188

Notes: K = magnetic susceptibility ($\times 10^{-6}$ SI units), NRM intensity = intensity of natural remanent magnetization, Q = Koenigsberger ratio, Inclination = stable inclination after demagnetization, P = anisotropy factor, K_1 and K_3 = maximum and minimum principal axes of susceptibility ellipsoid.

Table 2. Magnetic properties of peridotite recovered from Hole 897D.

Core, section, interval (cm)	Depth (mbsf)	NRM intensity ($\times 10^{-1}$ A/m)	Declination (°)	Inclination (°)	K ($\times 10^{-6}$ SI)	Q ratio	$P = K_1/K_3$
149-897D-							
11R-1, 69–71	694.49	3.12	202.1	14.5	15550	0.56	1.096
11R-2, 10–12	695.37	5.62	168.5	−69.9	19960	0.786	1.067
12R-1, 44–46	703.94	1.85	195.1	−22.1	15290	0.338	1.149
12R-4, 88–90	708.56	0.877	101.7	44.3	16580	0.148	1.077
13R-1, 62–64	713.62	5.68	157.8	20.6	14940	1.061	1.057
13R-5, 65–67	718.72	3.36	211.2	−23.9	12420	0.75	1.041
14R-3, 117–119	726.71	2.57	193.5	18.1	30750	0.233	1.106
15R-2, 86–88	734.5	5.04	352.4	44.4	24560	0.572	1.245
16R-2, 72–74	743.15	1.8	64.7	−52.1	26770	0.188	1.217
16R-3, 30–32	743.96	2.06	40	−31.9	12120	0.474	1.088
16R-3, 42–44	744.08	3.15	34.9	−35	7171	1.226	1.086
16R-4, 63–65	745.78	2.58	245.2	−2.3	20100	0.358	1.061
16R-5, 61–63	747.2	2.12	349.3	49.6	20920	0.283	1.123
17R-3, 26–28	754.86	3.81	171.3	−32.3	25360	0.419	1.052
17R-4, 14–16	755.81	0.29	170	−34.8	1254	0.645	1.073
17R-4, 118–120	756.85	0.32	155.7	−16.4	3123	0.286	1.036
17R-5, 7–9	757.1	0.27	160.9	−18.4	1746	0.432	1.03
17R-6, 15–17	757.93	0.78	160.8	−24.1	8652	0.252	1.059
18R-1, 10–12	761.36	0.21	201.5	−38.5	32390	0.018	1.056
18R-1, 16–18	763.24	0.14	245.1	−40.4	31960	0.012	1.053
19R-2, 58–60	772.69	1.1	168.6	33.4	14280	0.215	1.184
20R-1, 118–120	781.78	9.24	357.4	23.2	38080	0.677	1.223
20R-2, 135–137	783.42	7.39	2.9	−37.8	36690	0.562	1.104
21R-2, 16–18	791.1	4.61	327.7	10	23910	0.538	1.158
23R-3, 35–37	812.07	3.6	195.5	−10.5	25500	0.394	1.342
23R-4, 79–81	813.9	3.87	150.8	2	28890	0.374	1.201
23R-5, 31–33	814.84	7.56	319.5	5.4	30440	0.693	1.538
23R-5, 78–80	815.31	4.38	43	−26.3	37030	0.33	1.44
23R-6, 44–46	816.34	3.66	62.4	1.7	25150	0.406	1.253
24R-1, 88–90	819.48	1.05	205.5	−11.5	5805	0.505	1.306
24R-3, 57–59	821.29	2.17	315.4	38.5	22560	0.269	1.267
24R-4, 63–65	822.81	1.23	85.7	18.3	43860	0.079	1.349
25R-1, 20–22	828.4	1.34	162.2	−4.7	8304	0.45	1.155

Notes: K = magnetic susceptibility ($\times 10^{-6}$ SI units), NRM intensity = intensity of natural remanent magnetization, Q = Koenigsberger ratio, Inclination = stable inclination after demagnetization, P = anisotropy factor, K_1 and K_3 = maximum and minimum principal axes of susceptibility ellipsoid.

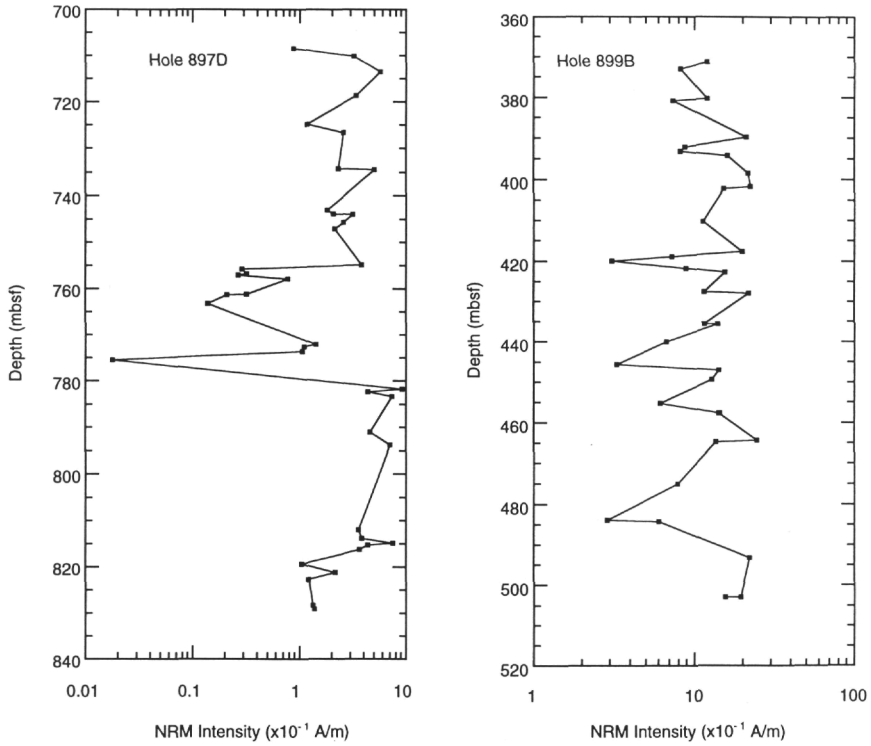

Figure 4. Intensity of NRM plotted against depth in Holes 897D and 899B.

termediate, and minimum susceptibilities (K_1, K_2, and K_3, respectively). These quantities are combined in various ways to describe different features of the ellipsoid and of the magnetic fabric it represents (Hrouda, 1982). AMS in peridotites most likely arises from the preferred orientation of anisotropic magnetic minerals (MacDonald and Ellwood, 1988). It is probable that net preferred alignment can be enhanced in these rocks by massive flow during emplacement. Thus, AMS is possibly relevant to distinguishing between emplacement modes. The ratio K_1/K_3 (P in Tables 1, 2) is commonly used as a measure of the degree of anisotropy. In the studied samples it is very low, ranging from 1.010 to 1.261 in Hole 899B and from 1.030 to 1.267 in Hole 897D (with five exceptions in the lowest part of the section, see Fig. 9), which suggests that there is very little anisotropy in the samples. The values of the anisotropy factor P at both holes show a pattern similar to the magnetic susceptibility. Under the assumption that cooling of these peridotites was contemporaneous with the emplacement, the AMS results would then suggest that the emplacement process of these rocks was probably not under a strong stress field.

Magnetic Polarity

In this study, polarity sense can be assigned with reasonable assurance on the basis of the inclination determined from discrete sample. The most exciting though unexpected result generated from this study is the identification of magnetic polarity zones in the peridotites. As shown in Figure 10, the inclinations of characteristic magnetization in the fresher lower part of the peridotite section are stable and show a consistent polarity pattern in a depth zone of about 21m. In Hole 897D, this zone starts at 743.15 mbsf (Sample 149-897D-16R-2, 72-74 cm), which corresponds to the onset depth of the fresher lower part of the section, and ends at 763.24 mbsf (Sample 149-897D-18R-1, 16-18 cm). In Hole 899B, it ranges from 435.72 mbsf (Sample 149-899B-23R-1, 12-14 cm) through 457.81 mbsf (Sample 149-899B-25R-3, 34-36 cm) and also coincides with the first appearance of greenish, fresher peridotites in the lower part of the section. At both holes, the inclinations of samples are predominantly negative (reversed) within this zone. In contrast, the inclinations of samples from the more "oxidized" upper part are almost all positive (normal).

There is also a difference in mean inclination between the two holes. In Hole 897D, the mean inclination for the upper part is 30.2° (N = 5, a_{95} = 20.5°, k = 19.4) and the mean inclination in the lower part is -31.4° (N = 12, a_{95} = 10.8°, k = 16.5). In Hole 899B, the mean inclination in the upper part is 22.6° (N = 20, a_{95} = 9.5°, k = 11.3) and for the lower part the mean inclination is -20.1° (N = 8, a_{95} = 8.3°, k = 49.2). These mean inclinations are significantly shallower than both that of present-day field (~64°) and those calculated from Cretaceous to Tertiary reference paleopoles for Europe, Africa, and North America, which range from 40.3° to 51.7° (see Van der Voo, 1993, p. 136, for the reference paleopoles).

Two observations of the paleomagnetic data from Site 897 are worth mentioning:

1. Several samples from the top of the altered upper part display negative inclinations (hence, reversed polarity?), suggesting that the normal polarity magnetization in the altered upper part was probably not a Holocene overprint. The most diagnostic examples are shown in Figure 11: a light-colored clayey limestone Sample 149-897C-66R-4, 15-17 cm, which was assigned a Late Cretaceous age based on the preliminary shipboard biostratigraphic ages, as well as a peridotite Sample 149-897D-11R-4, 71-73 cm, are both reversely magnetized. Similarly, indications for this reversed signal are present in peridotite Samples 149-897D-11R-2, 10-12 cm, and 149-897D-12R-1, 44-46 cm, at 695.37 and 703.94 mbsf, respectively (Table 2).
2. There is a possible narrow normal polarity interval at 747.2 mbsf in Hole 897D in which no obvious physical disturbance is present. It appears that this polarity transition is represented simultaneously in both inclination and declination, although the declination shows some additional shifts owing to the lack of internal orientation of these cores upon coring. It is also interesting to note that below this transition cores have the weakest NRM intensities within the basement section (see Table 2). These features, if true, would increase our confidence in the polarity determinations for both the upper and lower parts of the peridotite sections.

DISCUSSION

The rock magnetic properties of the peridotites are generally characterized by relatively strong NRM intensities and low Koenigsberger ratios. The average intensity of the recovered serpentinized peridotite is 0.29 A/m for samples from Hole 897D, but about 1.28 A/m for samples from Hole 899B. A recent magnetic survey revealed a magnetic anomaly high (about 0.3 A/m) in the vicinity of Site 899, which was previously thought to result from a relatively strongly magnetized nonoceanic crust (Whitmarsh et al., this volume). The much stronger magnetization intensity of Site 899 is apparently in excellent agreement with this observed magnetic anomaly high, suggesting that the serpentinized peridotite body under Site 899 contributes significantly to the magnetic anomaly. Conversely, the fact that Site 897 is located more oceanward, but has a mean NRM intensity less than one-third of the average intensity (~4 A/m) of dredged and drilled oceanic basalts in the Atlantic (Lowrie, 1977), may be used to explain the weakly negative anomaly data observed nearby.

The AMS data suggest that there is no noticeable magnetic anisotropy, and hence, probably no magneto-petrofabrics in these peridotites. This observation is consistent with other types of data, including data obtained by X-ray texture goniometry methods that indicate that there is little variation of fabrics in these peridotites (Morgan, this volume) and by seismic methods that suggest a weak degree of anisotropy (only about 7%) in these rocks (Harry and Batzle, this volume). These consistent observations would attest to the hypothesis that the peridotites were not strongly influenced by the extensional stress field that may prevail in the adjacent continental lithosphere.

Stable components of magnetization are revealed in the results of demagnetization on the peridotites from both holes. In the upper part, the remanence is dominated by a single stable component of normal polarity. Nearly identical directions of this component were found in all samples regardless of lithology and depth. Therefore, the paleomagnetic data of the altered upper part seem best interpreted as indicating that the magnetization is an overprint that was probably imposed during the alteration of these peridotites. The mean inclination of this overprinted magnetization is consistently shallower (~30°) than that of a Holocene field (~60°), suggesting that the overprint was unlikely acquired in the latter. In view of the polarity of magnetization identified from the overlying Cretaceous (see Fig. 11 for an example) and Tertiary sediments at both sites (Zhao et al., this volume), this normal overprint is probably older than the magnetization of the overlying Tertiary sediments.

In the fresher lower part, although the remanence is still dominated by a single component of magnetization in majority cases, several samples display a multicomponent nature, with a characteristic component isolated after removal of a secondary component of opposite polarity (Fig. 5). The characteristic component is carried by magnetite, which is known capable of preserving an early remanent magnetization over a long time. Because of the demagnetization behavior of these samples, I have no reason not to believe that the magnetization directions derived from these fresher peridotites are primary. Moreover, the reversed magnetization zone in the beginning of the fresher lower part is correlative between the two sites, which is perhaps the most compelling argument for the presence of primary magnetization because it would be difficult for a later remagnetization to produce such a preferential polarity pattern at depth. Several lines of overlapping evidence (Table 3) support my contention that the reversed magnetization zone in the beginning of the fresher lower part is correlative:

1. A distinctive increase in susceptibility was observed from shipboard pass-through magnetic susceptibility measurements at both sites (Fig. 12), which corresponds to the boundary between lithostratigraphic Units III and IV (Sawyer, Whitmarsh, Klaus, et al., 1994). The depth difference of this stratigraphic marker between the two sites is about 283 m.
2. Biostratigraphic and lithostratigraphic studies have determined that the unit boundaries between these two sites are also offset consistently by 285.4 m (see Sawyer, Whitmarsh, Klaus, et al., 1994; also see Fig. 2).
3. As mentioned, there is a Koenigsberger ratio peak found in both holes. Although this peak occurs in the more oxidized upper part and the value of the ratio itself does not carry much weight in the overall interpretation, its depth difference (291.7 m) between the two holes is significant, as it roughly coincides with the depth difference (307.4 m) of the reversed magnetic polarity zone found in the fresher lower part.

Therefore, these consistent markers of depth difference between the two sites indicate that the reversely magnetized peridotites in both holes are probably the same unit and recorded the same geomagnetic field during the time of emplacement.

Assuming the origins of the identified magnetic components of the peridotites are correctly established, the next step is to correlate the pattern of polarity changes with the established magnetic reversal sequence. To do so, it may be useful to briefly mention the marine magnetic Anomaly M0 and to review the proposed kinematic evolution and timing of important tectonic events among the major plates (Iberia, North America, Europe, and Africa) bordering the North Atlantic.

Marine magnetic anomalies have provided the richest source of information about magnetic reversals. The main reason for the high fidelity of the marine magnetic record is the remarkable continuity of the geologic processes by which new crust is formed along mid-ocean ridges. The polarity chrons of the pre-Aptian sequence are generally described by the M-sequence with designations "M0" through "M29" (Kent and Gradstein, 1985; Channell et al., 1987). There is still no direct isotopic dating of the M-sequence anomalies. The ages assigned by Kent and Gradstein (1985) to the M-sequence anomalies are based on fixing the Barremian/Aptian boundary at 118 Ma and the Oxfordian/Kimmeridgian boundary at 156 Ma. A number of short-period reversed events have been identified within the Cretaceous interval of dominantly normal polarity. The best documented of these is the reversed polarity event, of possible ~1 Ma duration, situated close to the Barremian/Aptian boundary (Hellsey and Steiner, 1969; McElhinny and Burek, 1971; Pechersky and Khramov, 1973; Channell et al., 1987). This reversal has been correlated with marine Anomaly M0. The M0 used in Kent and Gradstein's (1985) time scale is at 118 Ma, which immediately precedes the Cretaceous Long Normal Superchron (84-118 Ma). As most published papers about Iberia use this system, I adhere to the Kent and Gradstein (1985) time scale in this study.

Kinematic models for present-day plate motions (Minster and Jordan, 1978; Argus et al., 1989) and the distribution of earthquakes show that Iberia is now moving as part of Eurasia. However, continental geology strongly suggests that Iberia could not have moved with Eurasia during the formation of the Pyrenees in the Early Cretaceous (Srivastava et al., 1990). Paleomagnetic results on land also suggest that Iberia has rotated counterclockwise about 35° relative to Europe between the Barremian or Aptian and the Maastrichtian (Van der Voo, 1969, 1993) and that most of the rotation (30°) occurred at about Hauterivian to Aptian time (Galdeano et al., 1989). Several plate tectonic reconstructions have been attempted to show the original positions of North America, Iberia, and Europe (Le Pichon et al., 1977; Srivastava et al., 1990; Srivastava and Verhoef, 1992). At present, only models with marine magnetic data have the potential to provide estimates of the age of important events (although these events have to relate strictly to the history of seafloor spreading). By matching synchronous magnetic lineations and fracture zone systems that characterize the seafloor-spreading history between Europe and North America, Srivastava et al. (1990) reconstructed the history of Iberia's motion relative to its neighboring plates from Anomaly M0 (118 Ma on the time scale of Kent and Gradstein, 1985) to the present.

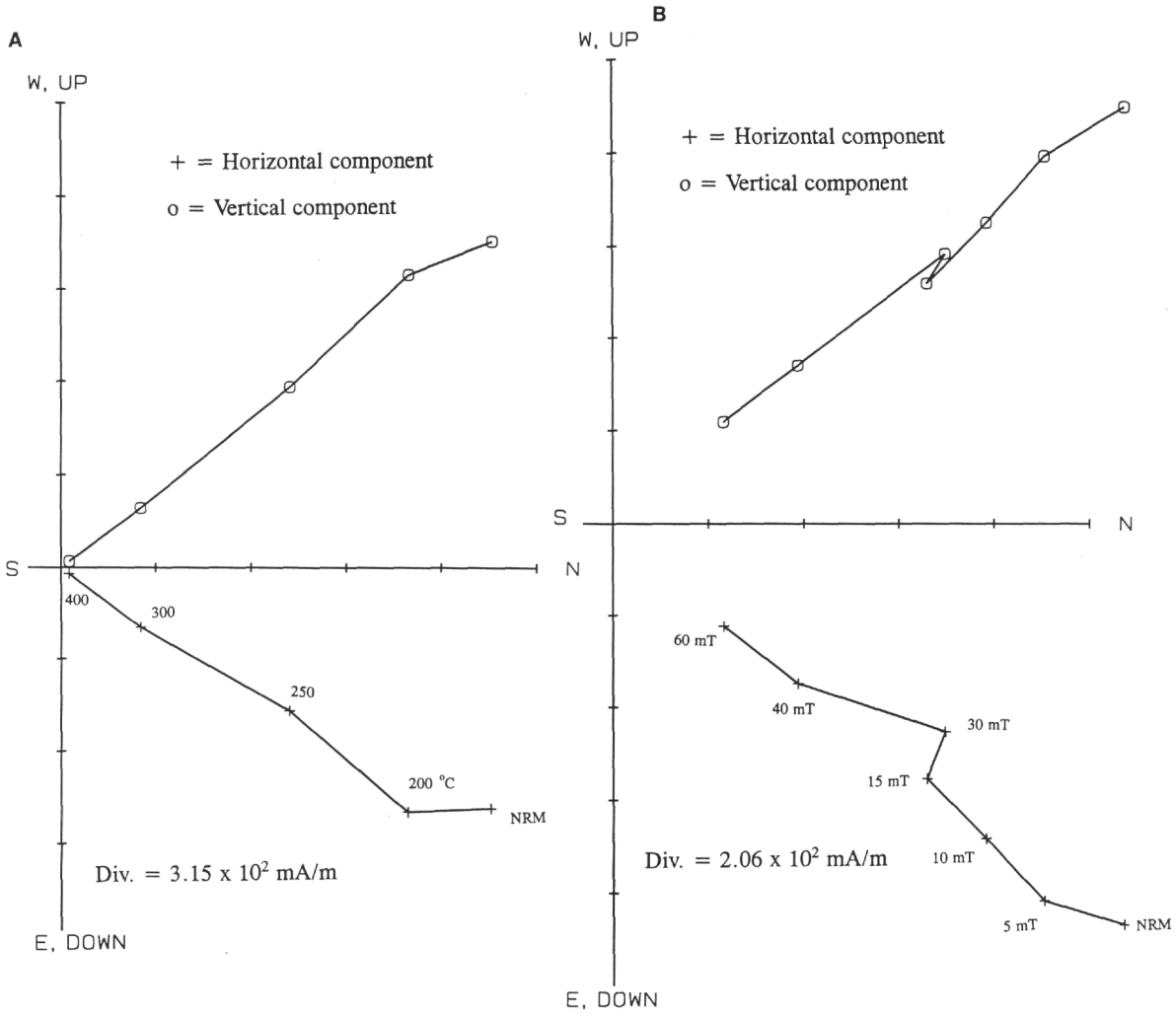

Figure 5. Representative vector end-point diagrams showing the results of thermal and alternating field demagnetization for samples from the "fresher" lower part of the peridotite section in Holes 897D and 899B. Reversed polarity of magnetization is revealed in all samples. **A.** Sample 149-897D-16R-3,42-44 cm. **B.** Sample 149-897D-16R-3, 30-32 cm. **C.** Sample 149-899B-23R-1, 12-14 cm. **D.** Sample 149-897D-16R-2, 72-74 cm. Plus signs and circles represent the projection of the magnetization vector end-point on the horizontal and vertical planes, respectively. NRM = natural remanent magnetization. Note that Samples 149-897D-16R-3. 42-44 cm, (A) and 149-897D-16R-3, 30-32 cm, (B) were taken from same piece of continuous core section.

They implied that Iberia was alternately attached to Africa or Europe and the opening of the North Atlantic was not an instantaneous process. Several salient features stand out from their kinematic model:

1. For the major part of the Cretaceous magnetic quiet period, Iberia moved as an independent plate.
2. Sometime before Chron 34 (84 Ma), Iberia became attached to the African plate, and the plate boundary between Africa and Eurasia was located at the Bay of Biscay.
3. From Chrons 34 (84 Ma) through 18 (42 Ma), Iberia was part of the African plate.
4. From the late Eocene (Chron 18, 42 Ma) to the early Miocene (Chron 6c, 24 Ma), Iberia again moved as an independent plate. The boundary between Eurasia and Iberia during this time extended west from the Pyrenees to King's Trough. The separation process is further complicated by intraplate deformation. The relative motion between Iberia and North America was transformed into the left-lateral motion of Iberia with respect to Europe (Le Pichon et al., 1977), and evidence of southwesterly motion of Iberia with respect to Europe was found in the fault pattern of the sedimentary basins north of Spain (Lepvrier and Martinez Garcia, 1990). 5. At about early Miocene (Chron 6c, 24 Ma) time, motion along the King's Trough/Azores-Biscay Rise boundary became very small, and Iberia started to move as part of the Eurasian plate (Srivastava et al., 1990).

The general evolution of the North Atlantic is now well documented in the literature (Bullard et al., 1965; Le Pichon et al., 1977; Courtillot, 1982; Srivastava and Tapscott, 1986; Klitgord and Schouten, 1986; Rowley and Lottes, 1988; Srivastava et al., 1990; Srivastava and Verhoef, 1992). Three rift-drift episodes can be recognized. The separation of Africa and North America is the oldest, with a Triassic-Jurassic rifting phase and a final breakup in the Middle Jurassic. The next phase is the separation of Iberia and the Grand Bank, which took place during the Early Cretaceous, with breakup at about 130 Ma. The last phase of seafloor spreading started with the separation of Europe from North America in the middle Cretaceous. Steady-state seafloor spreading between the Grand Bank and Iberia started at M0 time (118 Ma).

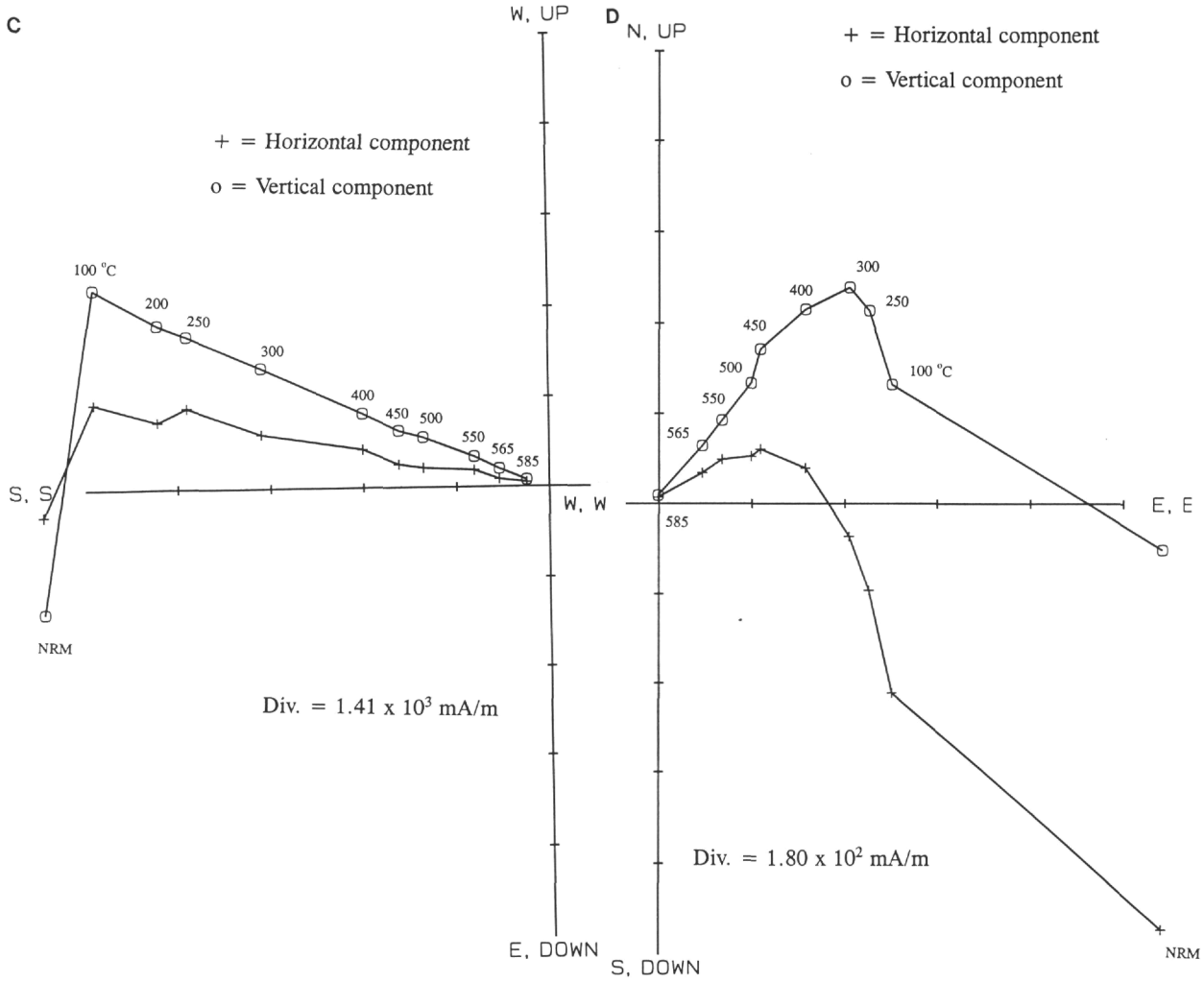

Figure 5 (continued).

Returning now to the age assignment of the polarity patterns identified from this study, I first want to point out that Leg 149 drilling successfully confirmed the timing of the second phase of the above-mentioned rift-drift episodes, originally proposed by Whitmarsh et al. (1990), in which Iberia started to drift in late Hauterivian time (M4, ~130 Ma), about 12 Ma earlier than the adjacent Galicia Bank. It is generally believed that continental breakups initiating ocean basins are preceded by a period of lithospheric stretching lasting about 20-50 Ma (Cochran, 1983), and the onset of oceanic spreading is assumed to be contemporaneous with the end of rifting and extensional tectonics on the margins (Malod and Mauffret, 1990). Therefore, it seems that the emplacement of Leg 149 peridotites probably occurred during the continental rifting and breakup of Iberia from the Grand Bank in late Hauterivian time (M4), and the observed reversed magnetization zone in the fresher lower part of the peridotite section most probably coincides with the onset of seafloor spreading between the Grand Bank and Iberia at M0 time (118 Ma). Because Anomaly M0 lasted only about 1 Ma, the overprinted normal magnetization signal observed in the more oxidized upper part of the peridotite section could be imposed any time within the Cretaceous Long Normal Superchron (84-118 Ma), most likely soon after the M0 time. These interpretations are fully consistent with the time constraints from the magnetic signatures of the overlying Cretaceous sediments, as mentioned above. The most conspicuous feature of the polarity records for the Cretaceous red and brown clays is a short reversed polarity zone, which may suggest that the deposition of these cores occurred during the M0 subchron.

Several lines of geological observations agree with the above age assignments to the magnetic polarity zones:

1. Biostratigraphic arguments suggest that the oldest units of these peridotites are Early Cretaceous in age (Hauterivian, about 135-132 Ma), and the first sediment deposited on top of the peridotite section was found to be Late Cretaceous in age. Therefore, the entire peridotite section should have been emplaced during the Cretaceous. Recent micropaleonotologic dating of cores from Hole 899B revealed that the emplacement of these peridotites probably lasted only about 1-2 Ma (de Kaenel and Bergen, this volume).
2. Magnetic Anomaly M0 is identified from only the east side of the peridotite sites (less than 150 km), suggesting the peridotites are of approximately the same age as Anomaly M0 (118 Ma).
3. Numerous major unconformities (at about 118 Ma) in many sedimentary basins surrounding the peridotite sites are concurrent with seafloor spreading at M0 time. On the Iberian margin side, these tectonostratigraphic basins include the Inner Galicia Basin (Murillas et al., 1990) and Lusitanian Basin (Wilson et al., 1989), and on the Newfoundland side, the Whale Basin (Balkwill and Legall, 1989) and Jeanne d'Arc Basin (Tankard

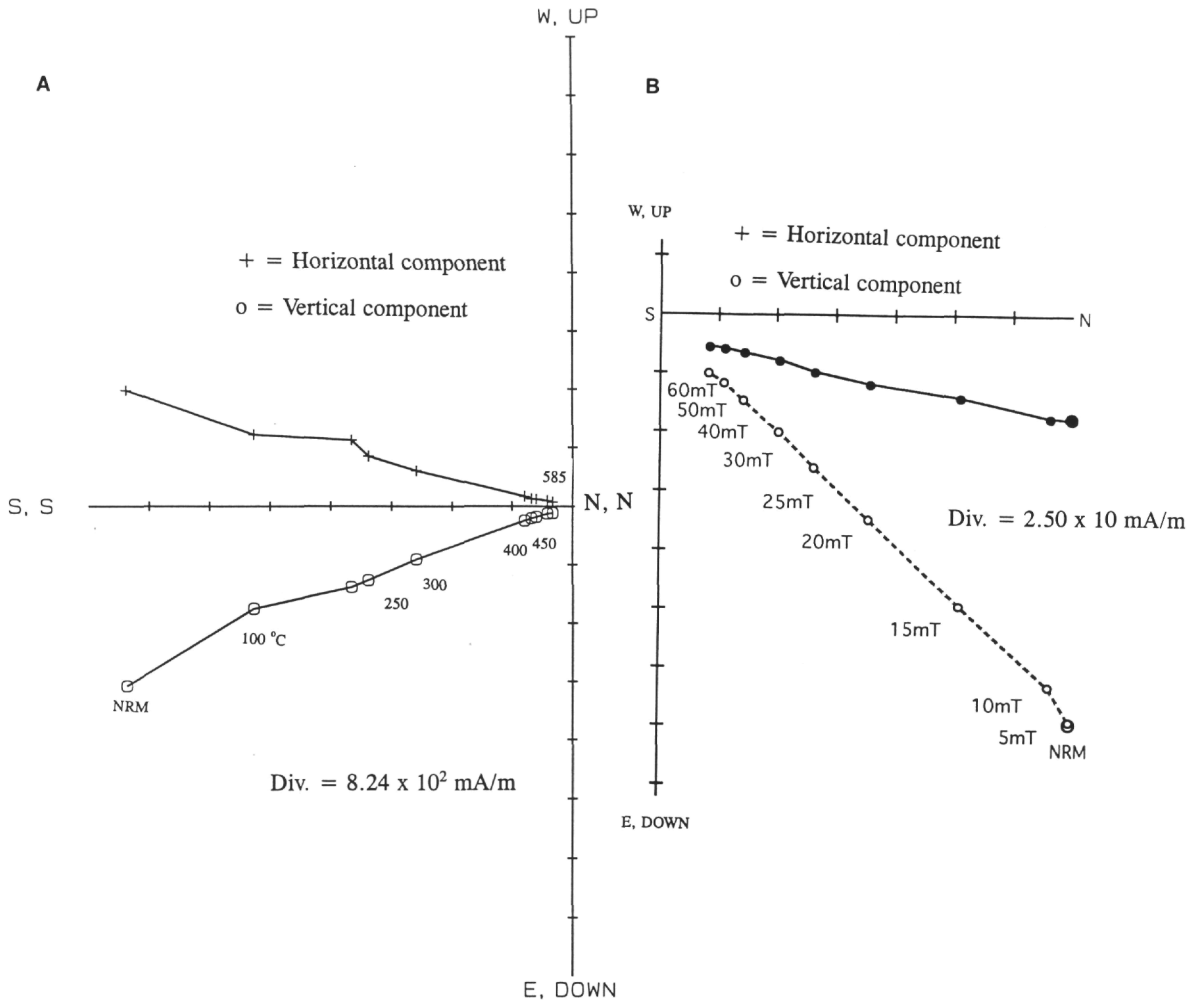

Figure 6. Representative vector end-point diagram showing the results of thermal and alternating field demagnetization for samples from the "altered" upper part of the peridotite section. Normal polarity of magnetization is revealed in all samples. **A.** Sample 149-899B-16R-3, 57-59 cm. **B.** Sample 149-899B-21R-4, 77-79 cm. **C.** Sample 149-899B-20R-2, 112-114 cm. **D.** Sample 149-899B-21R-2, 75-77 cm. Conventions as in Figure 5. Sample 149-899B-20R-2, 112-114 cm, (C) was specifically taken from a heavily veined core section, whereas Samples 149-899B-16R-3, 57-59 cm, (A) and 149-899B-21-2, 75-77 cm, (D) were from relatively vein-free pieces.

et al., 1989). These unconformities not only provide a direct linkage between the evolution of these basins and separation of Iberia from North America, but also suggest that the emplacement and alteration events in these peridotites should have taken place at about M0 time.

4. Shipboard observations suggest that the alteration of the peridotites recovered during Leg 149 took place soon after the peridotites were emplaced at or near the seafloor surface and that the fluid responsible for serpentinization was probably seawater. Therefore, both the paleomagnetic and geologic data are compatible with the suggestion that alteration by fluid circulation was associated with the first stages of accretion of the oceanic crust, during the middle Cretaceous.

It is beyond the scope of this paper to propose a detailed and quantitative model for the emplacement process of the peridotites recovered during Leg 149. However, it is appropriate to discuss qualitatively some of the constraints from paleomagnetic data and other relevant geologic data that can be placed on the potential models for the mode of emplacement and the late-stage alteration of these peridotites.

The sites at which peridotite was recovered during Leg 149 are regions where the crust is missing and where the mantle rocks crop out directly on the seafloor. This would imply that progressive uplift and final emplacement of peridotites at the Earth's surface seem to be related to the thinning of the continental crust beneath the rift. As mentioned in the "Introduction" section, several distinct models have been proposed to account for the uplift of mantle rocks on the seafloor in relation to continental rifting. These models include diapiric emplacement (Nicolas et al., 1987; Bonatti, 1987) and tectonic denudation by detachment faulting (Boillot et al., 1987). Although both models can be used to explain the exposure of upper mantle rocks at the end of the rifting, they both pose certain difficulties when applied to the peridotites at Iberia margin. Specifically, the vertical asthenosphere diapiric model predicts basalt flow should exist on top of the "diapirs," and the detachment faulting model requires that the mantle rocks experience ductile deformation at great depth and brittle deformation near the surface. Shipboard petrologic observations found a complete absence of basaltic clasts within the serpentinized peridotites at both Holes 897D and 899B. Therefore, the vertical diapirism model cannot completely account for the emplacement process at these sites. On the other hand, the current lack of evidence for the

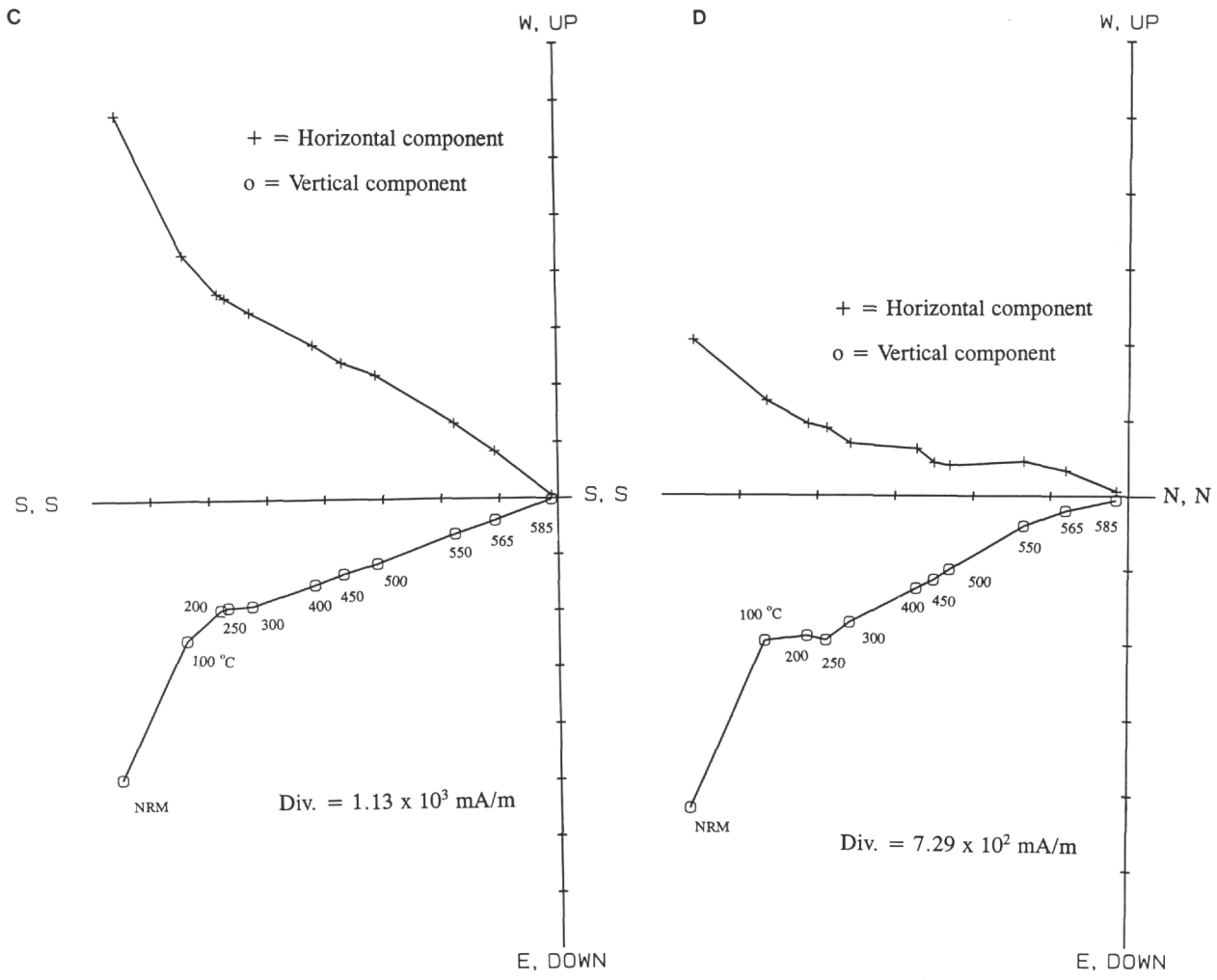

Figure 6 (continued).

presence of anisotropy in these peridotites, as indicated by the AMS data from this study, would pose some difficulties for a pure detachment faulting model. Because uplift of the peridotite by some kind of diapiric mechanism is needed and detachment faulting accounts nicely for the crustal thinning and stretching, I propose a combination of these two models for the process of emplacement of the Iberian peridotites. Uplift by diapirism could occur prior to the main stage of stretching. At the end of the stretching phase, when the crust is particularly thinned, these peridotites would be serpentinized by seawater circulation (which is responsible for remagnetizing the upper part of the peridotites) and hence become less dense than the surrounding crustal material. Finally, the serpentinized peridotites rose to the seafloor and cropped out at the ocean/continent boundary just before "true" seafloor spreading started between the Iberian and Newfoundland margins (i.e., the opening of North Atlantic).

CONCLUSIONS

The Iberian peridotites recovered from Holes 897D and 899B preserve a magnetic memory of the middle Cretaceous geomagnetic field and provide a rare opportunity for dating the tectonic processes that accompanied continental breakup and opening of the North Atlantic. The fresher peridotites have Cretaceous (shallow) inclinations and a reverse polarity and are therefore most likely pre-Cretaceous Long Normal Superchron. The altered zone still has these shallow inclinations but is predominantly normal. Because other work shows that alteration was early, the normal inclination is probably of Cretaceous Long Normal Superchron age. Magnetic polarity patterns identified at these two sites appear to suggest that the emplacement of these peridotites took place sometime during the middle Cretaceous (probably at M0 time, 118 Ma), and subsequent alteration of the upper part of these peridotites probably occurred during the Cretaceous Long Normal Superchron (most likely between 117 and 84 Ma) by seawater during the opening of the North Atlantic. These peridotites were probably brought up by a combination process of mantle upwelling and lithospheric stretching and reached the last stage of their evolution about 110 Ma ago.

ACKNOWLEDGMENTS

I thank the Joint Oceanographic Institutions, Inc. and the Ocean Drilling Program for enabling my participation on Leg 149. The scientific party and technical staff for Leg 149 provided valuable assistance and insights into this work. I wish to thank Drs. Randy Enkin and Stuart Gilder for providing valuable comments. I am also grateful to Professor Jose Honnorez for his thoughtful review and helpful comments. Special thanks go to Professor Rob Coe, who encouraged me to participate in ODP research and provided guidance during the study. Financial support for various part of this research was provided by a grant from the U.S. Science Advisory Committee and NSF

grant EAR 443226-21777. This is also Institute of Tectonics of University of California at Santa Cruz Contribution no. 269.

REFERENCES

Argus, D.F., Gordon, R.G., DeMets, C, and Stein, S., 1989. Closure of Africa-Eurasia-North America Plate motion circuit and tectonics of the Gloria fault. *J. Geophys. Res.,* 94:5585-5602.

Balkwill, H.R., and Legall, F.D., 1989. Whale basin, offshore Newfoundland: extension and salt diapirism. *In* Tankard, A.J., and Balkwill, H.R. (Eds.), *Extensional Tectonics and Stratigraphy of the North Atlantic Margins*. AAPG Mem., 46:233-246.

Beslier, M.-O., Girardeau, J., and Boillot, G., 1990. Kinematics of peridotite emplacement during North Atlantic continental rifting, Galicia, NW Spain. *Tectonophysics,* 184:321-343.

Boillot, G., Recq, M., Winterer, E., Meyer, A.W., Applegate, J., Baltuck, M., Bergen, J.A., Comas, M.C., Davis, T.A., Dunham, K., Evans, C.A., Girardeau, J., Goldberg, D.G., Haggerty, J., Jansa, L.F., Johnson, J.A., Kasahara, J., Loreau, L.-P., Luna-Sierra, E., Moullade, M., Ogg, J., Sarti, M., Thurow, J., and Williamson, M., 1987. Tectonic denudation of the upper mantle along passive margins: a model based on drilling results (ODP Leg 103, western Galicia margin, Spain). *Tectonophysics,* 132:335-342.

Bonatti, E., 1987. The rifting of continents. *Sci. Am.,* 258:96-103.

Bonatti, E., and Honnorez, J., 1976. Sections of Earth's crust in the equatorial Atlantic. *J. Geophys. Res.,* 81:4104-4116.

Bonatti, E., Ottonello, G., and Hamlyn, R.E., 1986. Peridotites of the Island of Zabargad (St. John), Red Sea: petrology and geochemistry. *J. Geophys. Res.,* 91:599-631.

Bullard, E., Everett, J.E., and Smith, A.G., 1965. The fit of the continents around the Atlantic. *Philos. Trans. R. Soc. London A,* 258:41-75.

Channell, J.E.T., Bralower, T.J., and Grandesso, P., 1987. Biostratigraphic corelation of Mesozoic polarity chrons CM1 and CM23 at Capriolo and Xausa (Southern Alps, Italy). *Earth Planet. Sci. Lett.,* 85:203-221.

Cochran, J.R., 1983. Effects of finite rifting times on the development of sedimentary basins. *Earth Planet. Sci. Lett.,* 66:289-302.

Courtillot, V., 1982. Propagating rifts and continental breakup. *Tectonics,* 1:239-250.

Galdeano, A., Moreau, M.G., Pozzi, J.P., Berthou, P.Y., and Malod, J.A., 1989. New paleomagnetic results from Cretaceous sediments near Lisboa (Portugal) and implications for the rotation of Iberia. *Earth Planet. Sci. Lett.,* 92:95-106.

Girardeau, J., Evans, C.A., and Beslier, M.-O., 1988. Structural analysis of plagioclase-bearing peridotites emplaced at the end of continental rifting: Hole 637A, ODP Leg 103 on the Galicia Margin. *In* Boillot, G., Winterer, E.L., et al., *Proc. ODP, Sci. Results,* 103: College Station, TX (Ocean Drilling Program), 209-223.

Hellsey, C.E., and Steiner, M.D., 1969. Evidence for long intervals of normal polarity during the Cretaceous period. *Earth Planet. Sci. Lett.,* 5:325-332.

Hrouda, F., 1982. Magnetic anisotropy of rocks and its application in geology and geophysics. *Geophys. Surv.,* 5:37-82.

Kent, D.V., and Gradstein, F.M., 1986. A Jurassic to Recent chronology. *In* Tucholke, B.E., and Vogt, P.R. (Eds.), *The Geology of North America: The Western Atlantic Region.* Geol. Soc. Am. DNAG Ser., 1:45-50.

Kirschvink, J.L., 1980. The least-squares line and plane and the analysis of palaeomagnetic data. *Geophys. J. R. Astron. Soc.,* 62:699-718.

Klitgord, K.D., and Schouten, H., 1986. Plate kinematics of the central Atlantic. *In* Vogt, P.R., and Tucholke, B.E. (Eds.), *The Geology of North America* (Vol. M): *The Western North Atlantic Region.* Geol. Soc. Am., 351-378.

Le Pichon, X., Sibuet, J.C., and Francheteau, J., 1977. The fit of the continents around the North Atlantic Ocean. *Tectonophysics,* 38:169-209.

Lepvrier, C., and Martinez Garcia, E., 1990. Fault development and stress evolution of the post-Hercynian Asturian basin (Asturias and Cantabria), northwestern Spain. *Tectonophysics,* 184:345-356.

Lowrie, W., 1977. Intensity and direction of magnetisation in oceanic basalts. *J. Geol. Soc. London,* 133:61-82.

Malod, J.A., and Mauffret, A., 1990. Iberian plate motion during the Mesozoic. *In* Boillot, G., and Fontbote, J.M. (Eds.), *Alpine Evolution of Iberia and its Continental Margins.* Tectonophysics, 184:261-278.

MacDonald, W.D., and Ellwood, B.B., 1988. Magnetic fabric of peridotite with intersecting petrofabric surfaces, Tinaquillo, Venezuela. *Phys. Earth Planet. Inter.,* 51:301-312.

McElhinny, M.W., and Burek, P.J., 1971. Mesozoic palaeomagnetic stratigraphy. *Nature,* 232:98-102.

Minster, J.B., and Jordan, T.H., 1978. Present-day plate motions. *J. Geophys. Res.,* 83:5331-5354.

Murillas, J., Mougenot, D., Boillot, G., Comas, M.C., Banda, E., and Mauffret, A., 1990. Structure and evolution of the Galicia Interior basin (Atlantic western Iberian continental margin). *Tectonophysics,* 184:297-319.

Nicolas, A., 1984. Lherzolites of the western Alps: a structural review. *In* Kornprobst, J. (Ed.), *Kimberlites II: the Mantle and Crust-Mantle Relationships:* Amsterdam (Elsevier), 333-345.

Nicolas, A., Boudier, F., and Montigny, R., 1987. Structure of Zabargad Island and early rifting of the Red Sea. *J. Geophys. Res.,* 92:461-74.

Nicolas, A., Boudier, F., Lyberis, N., Montigny, R., and Guennoc, P., 1985. Zabargad (St. John) Island: a key-witness of early rifting in the Red Sea. *C. R. Acad. Sci. Ser.* 2., 301:1063-1068.

Obata, M., 1977. Petrology and petrogenisis of the Ronda high-temperature peridotite intrusion, southern Spain [Ph.D. thesis]. Massachusetts Inst. Technology, Cambridge, MA.

Pechersky, D.M., and Khramov, A.N., 1973. Mesozoic palaeomagnetic scale of the USSR. *Nature,* 244:499-501.

Rochette, P., Jackson, M., and Aubourg, C., 1992. Rock magnetism and the interpretation of anisotropy of magnetic susceptibility. *Rev. Geophys.,* 30:209-226.

Rowley, D.B., and Lottes, A.L., 1988. Plate kinematic reconstructions of the North Atlantic and Arctic: Late Jurassic to present. *Tectonophysics,* 155:73-120.

Sawyer, D.S., Whitmarsh, R.B., Klaus, A., et al., 1994. *Proc. ODP, Init. Repts.,* 149: College Station, TX (Ocean Drilling Program).

Seifert, K.E., Gibson, I.L., and ODP Leg 149 Shipboard Scientific Party, 1993. ODP Leg 149 igneous rocks, Iberia Abyssal Plain. *Eos,* 74:623.

Srivastava, S.P., Roest, W.R., Kovacs, L.C., Oakey, G., Levesque, S., Verhoef, J., and Macnab, R., 1990. Motion of Iberia since the Late Jurassic: results from detailed aeromagnetic measurements in the Newfoundland Basin. *Tectonophysics,* 184:229-260.

Srivastava, S.P., and Tapscott, C.R., 1986. Plate kinematics of the North Atlantic. *In* Vogt, P.R., and Tucholke, B.E. (Eds.), *The Western North Atlantic Region.* Geol. Soc. Am., Geol, of North Am. Ser., M:379-404.

Srivastava, S.P., and Verhoef, J., 1992. Evolution of Mesozoic sedimentary basins around the North Central Atlantic: a preliminary plate kinematic solution. *In* Parnell, J. (Ed.), *Basins of the Atlantic Seaboard: Petroleum Geology, Sedimentology and Basin Evolution.* Geol. Spec. Publ. London, 62:397-420.

Tankard, A.J., Welsink, H.J., and Jenkins, W.A.M., 1989. Structure styles and stratigraphy of the Jeanne d'Arc basin, Grand Banks of Newfoundland. *In* Tankard, A.J., and Balkwill, H.R. (Eds.), *Extensional Tectonics and Stratigraphy of the North Atlantic Margins.* AAPG Mem., 46:265-282.

Tubia, S.M., and Cuevas, J., 1977. Structure et cinematique liée à la mise en place des peridotites de Ronda (Cordilleres Betiques, Espagne), *Geodin. Acta,* 1:59-69.

Van der Voo, R., 1969. Paleomagnetic evidence for the rotation of the Iberia peninsula. *Tectonophysics,* 7:5-56.

———, 1993. *Paleomagnetism of the Atlantic, Tethys and Iapetus Oceans:* Cambridge Univ. Press.

Vielzeuf, D., and Kornprobst, J., 1984. Crustal splitting and the emplacement of Pyrenean lherzolites and granulites. *Earth Planet. Sci. Lett.,* 67:87-96.

Whitmarsh, R.B., Miles, P.R., and Mauffret, A., 1990. The ocean-continent boundary off the western continental margin of Iberia, I. Crustal structure at 41°30'N. *Geophys. J. Inter.,* 103:509-531.

Wilson, R.C.L., Hiscott, R.N., Willis, M.G., and Gradstein, P.M., 1989. The Lusitanian Basin of west-central Portugal: Mesozoic and Tertiary tectonic, stratigraphic and subsidence history. *In* Tankard, A.J., and Balkwill, H.R. (Eds.), *Extensional Tectonics and Stratigraphy of the North Atlantic Margins.* AAPG Mem., 46:341-361.

Zijderveld, J.D.A., 1967. AC demagnetization of rocks: analysis of results. *In* Collinson, D.W., Creer, K.M., and Runcorn, S.K. (Eds.), *Methods in Palaeomagnetism:* New York (Elsevier), 254-286.

Date of initial receipt: 5 December 1994
Date of acceptance: 26 June 1995
Ms 149SR-214

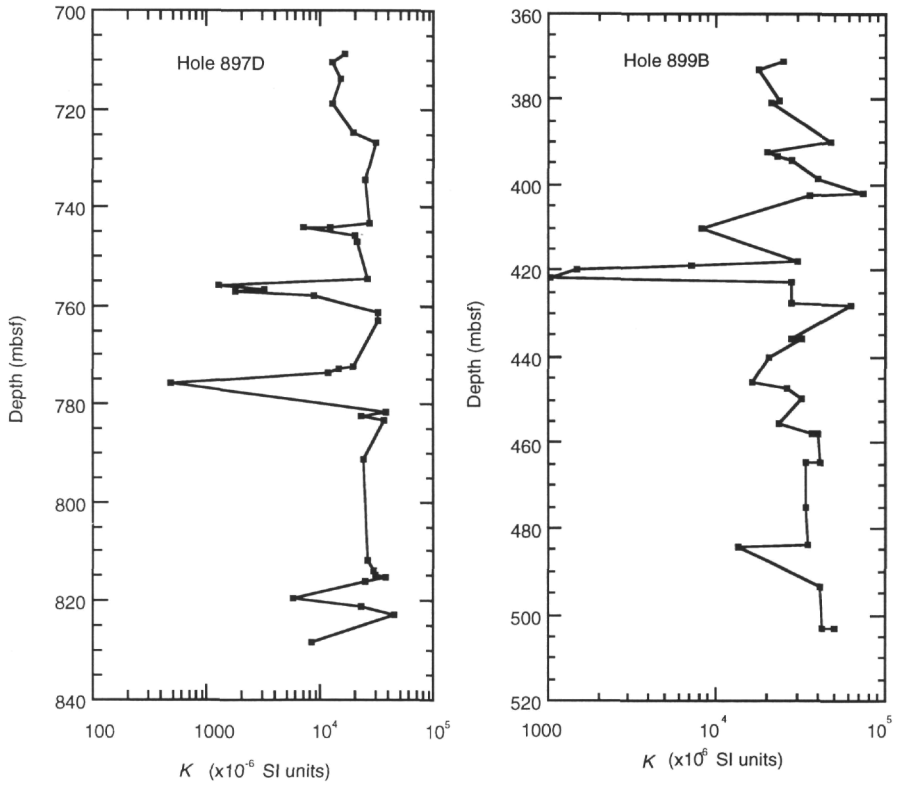

Figure 7. Magnetic susceptibility (× 10^{-6} SI units) of peridotite samples plotted against depth in Holes 897D and 899B.

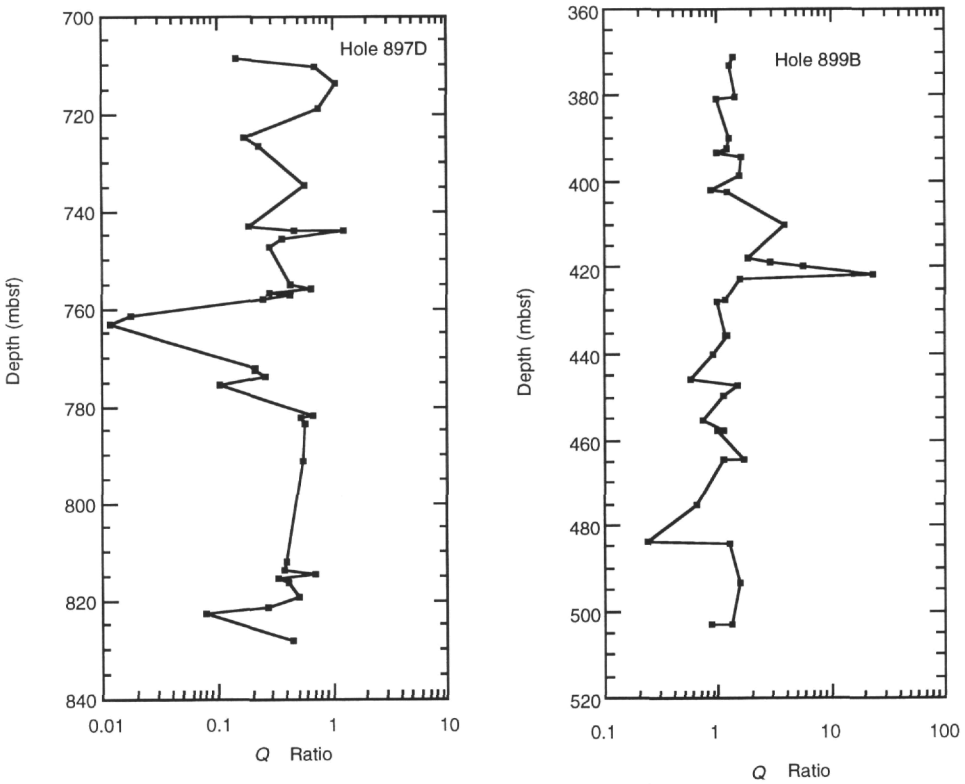

Figure 8. Koenigsberger ratio of peridotite samples plotted against depth in Holes 897D and 899B.

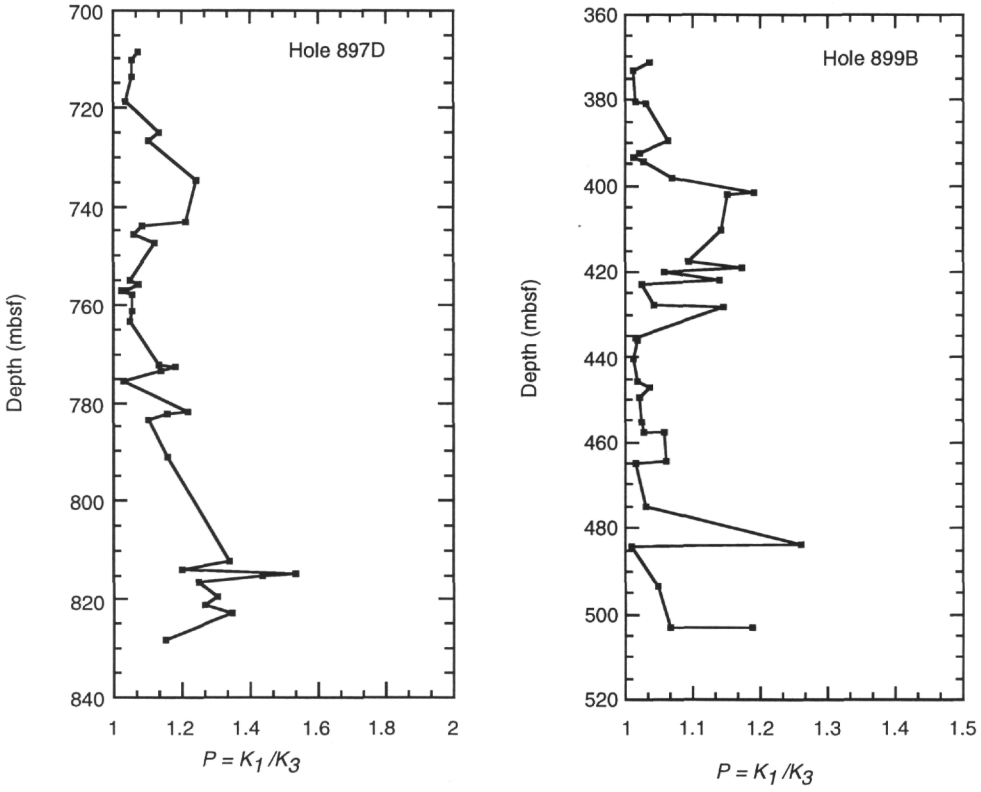

Figure 9. Anisotropy factor (P) of peridotite samples plotted against depth in Holes 897D and 899B.

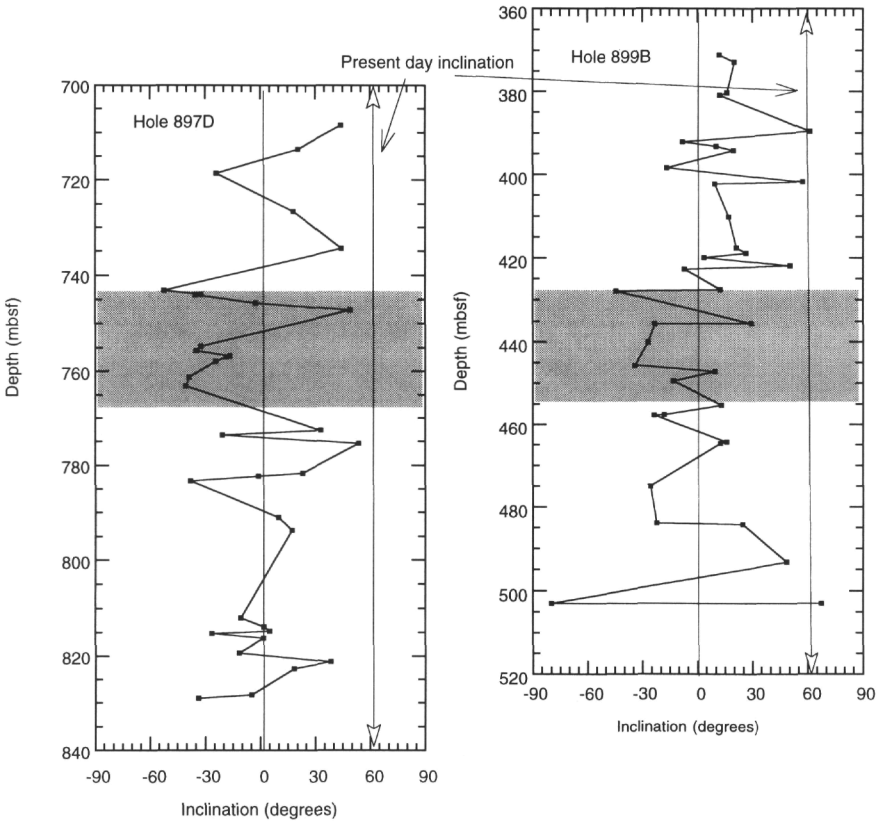

Figure 10. Inclinations of ChRM of peridotite samples plotted against depth in Holes 897D and 899B. Shaded areas correspond to the fresher lower part of the section. The present-day field inclination at the Leg 149 drilling sites is also indicated.

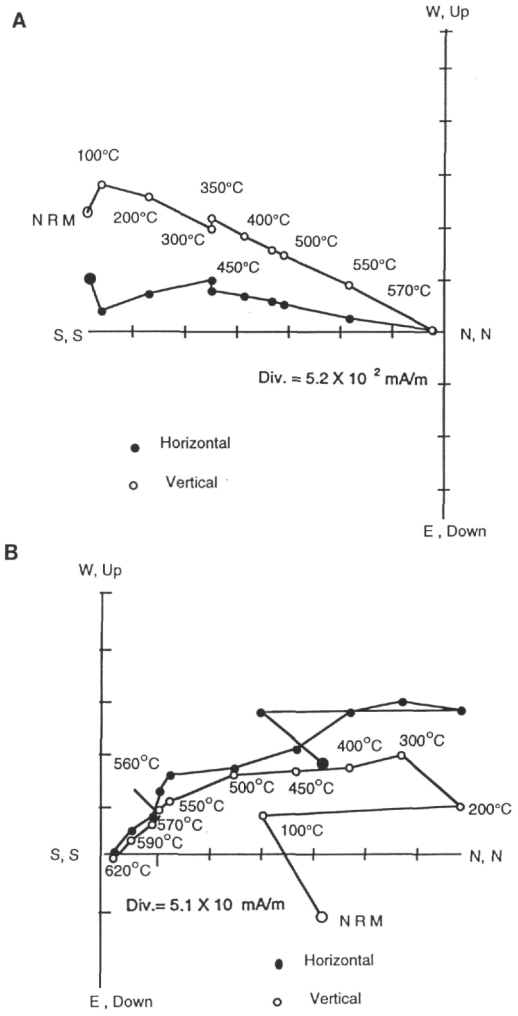

Figure 11. Orthogonal projections of thermal demagnetization results from cores overlying the altered upper part of the peridotite section at Site 897 show that the stable component of magnetization is probably of reversed polarity. **A.** Sample 149-897C-66R-4, 15-17 cm. **B.** Sample 149-897D-11R-4, 71-73 cm.

Table 3. Three overlapping observations for depth difference (mbsf) at Holes 897D and 899B.

Marker	Hole 897D	Hole 899B	Depth difference
Downhole susceptibility peak	647	364	283
Lithostratigraphic Unit IVA boundary	655.2	369.8	285.4
Q-ratio peak	713.6	421.9	291.7
Onset of the reversal zone	743.1	435.7	307.4

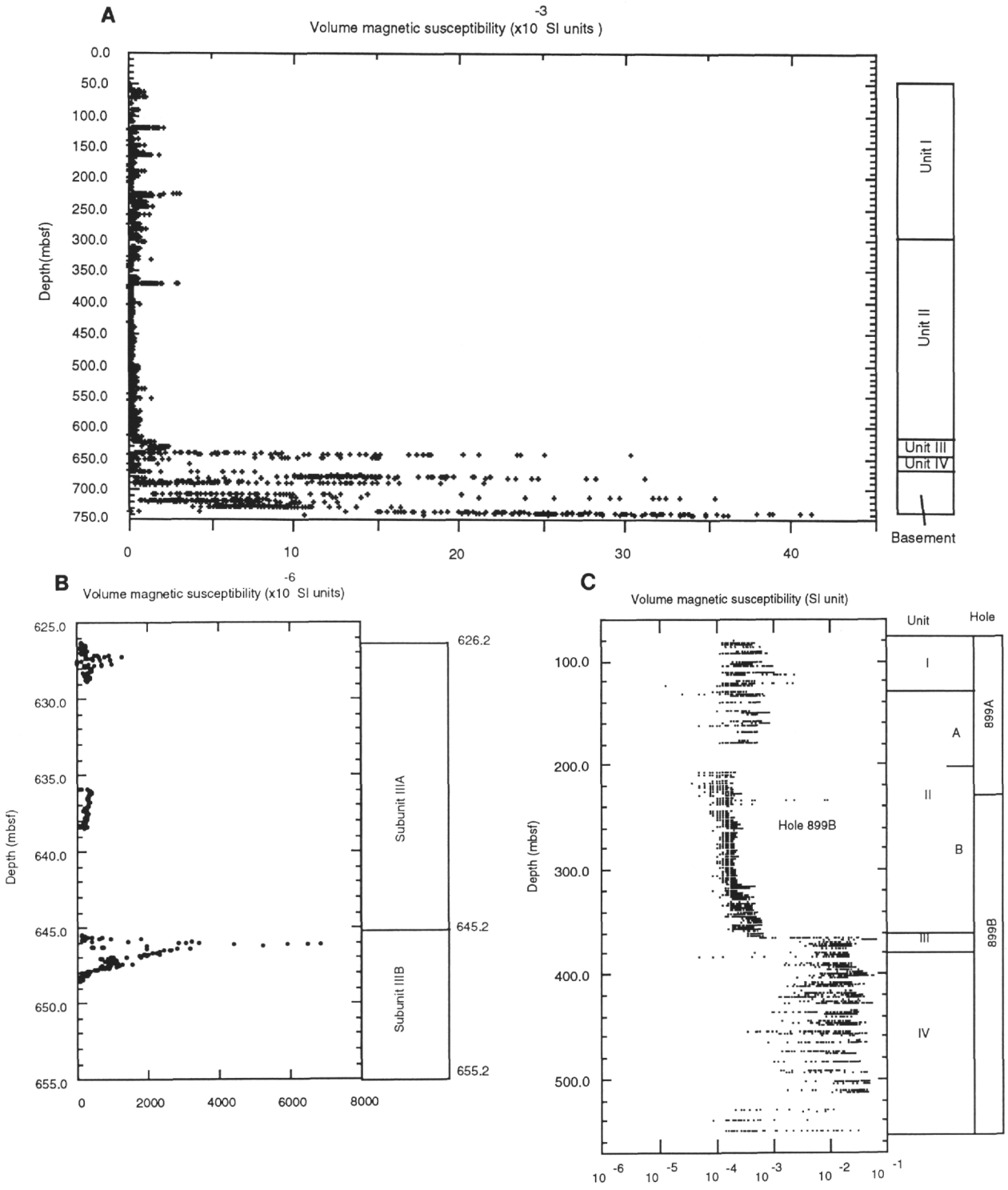

Figure 12. Whole-core magnetic susceptibility plotted as a function of depth from (**A**) Hole 897C, (**B**) Hole 897D, and (**C**) Hole 899B. Magnetic susceptibility was measured at 3- to 5-cm intervals on most of the recovered sedimentary and peridotite cores using the Bartington Instruments susceptibility meter (model MS 1; 80-mm loop, 4.7 kHz, SI units) mounted on the multisensor track aboard ship. Lithostratigraphic units are shown in the column to the right.